Research Article | Vol. 25, No. 22 | 30 Oct 2017 | OPTICS EXPRESS 26958
Optics EXPRESS

Sub-MW peak power diffraction-limited chirped-pulse monolithic Yb-doped tapered fiber amplifier

KONSTANTIN BOBKOV,[1] ALEXEY ANDRIANOV,[2] MAXIM KOPTEV,[2] SERGEY MURAVYEV,[2] ANDREI LEVCHENKO,[1] VLADIMIR VELMISKIN,[1] SVETLANA ALESHKINA,[1] SERGEY SEMJONOV,[1] DENIS LIPATOV,[3] ALEXEY GURYANOV,[3] ARKADY KIM,[2] AND MIKHAIL LIKHACHEV[1,*]

[1]*Fiber Optics Research Center of the Russian Academy of Sciences, 38 Vavilov Street, Moscow, 119333, Russia*
[2]*Institute of Applied Physics of the Russian Academy of Sciences, 46 Ulyanov Street, Nizhny Novgorod, 603950, Russia*
[3]*Institute of Chemistry of High Purity Substances of Russian Academy of Sciences, 49 Tropinin Street, Nizhny Novgorod, 603950, Russia*
[*]*likhachev@fo.gpi.ru*

Abstract: We demonstrate a novel amplification regime in a counter-pumped, relatively long (2 meters), large mode area, highly Yb-doped and polarization-maintaining tapered fiber, which offers a high peak power directly from the amplifier. The main feature of this regime is that the amplifying signal propagates through a thin part of the tapered fiber without amplification and experiences an extremely high gain in the thick part of the tapered fiber, where most of the pump power is absorbed. In this regime, we have demonstrated 8 ps pulse amplification to a peak power of up to 0.76 MW, which is limited by appearance of stimulated Raman scattering. In the same regime, 28 ps chirped pulses are amplified to a peak power of 0.35 MW directly from the amplifier and then compressed with 70% efficiency to 315 ± 10 fs, corresponding to an estimated peak power of 22 MW.

OCIS codes: (060.2280) Fiber design and fabrication; (060.2320) Fiber optics amplifiers and oscillators; (060.3510) Lasers, fiber.

References and links

1. T. Eidam, J. Rothhardt, F. Stutzki, F. Jansen, S. Hädrich, H. Carstens, C. Jauregui, J. Limpert, and A. Tünnermann, "Fiber chirped-pulse amplification system emitting 3.8 GW peak power," Opt. Express **19**(1), 255–260 (2011).
2. R. Sun, D. Jin, F. Tan, S. Wei, C. Hong, J. Xu, J. Liu, and P. Wang, "High-power all-fiber femtosecond chirped pulse amplification based on dispersive wave and chirped-volume Bragg grating," Opt. Express **24**(20), 22806–22812 (2016).
3. W. S. Wong, X. Peng, J. M. McLaughlin, and L. Dong, "Robust Single-Mode Propagation in Optical Fibers with Record Effective Areas," in *Conference on Lasers and Electro-Optics/Quantum Electronics and Laser Science and Photonic Applications Systems Technologies, Technical Digest (CD)* (Optical Society of America, 2005), paper CPDB10.
4. S. Ramachandran, J. W. Nicholson, S. Ghalmi, M. F. Yan, P. Wisk, E. Monberg, and F. V. Dimarcello, "Light propagation with ultralarge modal areas in optical fibers," Opt. Lett. **31**(12), 1797–1799 (2006).
5. L. Lavoute, P. Roy, A. Desfarges-Berthelemot, V. Kermène, and S. Février, "Design of microstructured single-mode fiber combining large mode area and high rare earth ion concentration," Opt. Express **14**(7), 2994–2999 (2006).
6. P. Wang, L. J. Cooper, J. K. Sahu, and W. A. Clarkson, "Efficient single-mode operation of a cladding-pumped ytterbium-doped helical-core fiber laser," Opt. Lett. **31**(2), 226–228 (2006).
7. C.-H. Liu, G. Chang, N. Litchinister, D. Guertin, N. Jacobson, K. Tankala, and A. Galvanauskas, "Chirally Coupled Core Fibers at 1550-nm and 1064-nm for Effectively Single-Mode Core Size Scaling," in *Conference on Lasers and Electro-Optics/Quantum Electronics and Laser Science Conference and Photonic Applications Systems Technologies, OSA Technical Digest Series (CD) (Optical Society of America, 2007)*, paper CTuBB3.
8. D. A. Gaponov, S. Février, M. Devautour, P. Roy, M. E. Likhachev, S. S. Aleshkina, M. Y. Salganskii, M. V. Yashkov, and A. N. Guryanov, "Management of the high-order mode content in large (40 microm) core photonic bandgap Bragg fiber laser," Opt. Lett. **35**(13), 2233–2235 (2010).
9. L. Daniault, D. A. Gaponov, M. Hanna, S. Février, P. Roy, F. Druon, P. Georges, M. E. Likhachev, M. Y. Salganskii, and M. V. Yashkov, "High power femtosecond chirped pulse amplification in large mode area photonic bandgap Bragg fibers," Appl. Phys. B **103**(3), 615–621 (2011).

#300439 https://doi.org/10.1364/OE.25.026958
Journal © 2017 Received 20 Jun 2017; revised 13 Oct 2017; accepted 15 Oct 2017; published 20 Oct 2017

10. P. K. Mukhopadhyay, K. Ozgoren, I. L. Budunoglu, and F. O. Ilday, "All-Fiber Low-Noise High-Power Femtosecond Yb-Fiber Amplifier System Seeded by an All-Normal Dispersion Fiber Oscillator," IEEE J. Sel. Top. Quantum Electron. **15**(1), 145–152 (2009).
11. H. Kalaycioglu, B. Oktem, C. Şenel, P. P. Paltani, and F. Ö. Ilday, "Microjoule-energy, 1 MHz repetition rate pulses from all-fiber-integrated nonlinear chirped-pulse amplifier," Opt. Lett. **35**(7), 959–961 (2010).
12. V. Filippov, Y. Chamorovskii, J. Kerttula, K. Golant, M. Pessa, and O. G. Okhotnikov, "Double clad tapered fiber for high power applications," Opt. Express **16**(3), 1929–1944 (2008).
13. Y. Jung, Y. Jeong, G. Brambilla, and D. J. Richardson, "Adiabatically tapered splice for selective excitation of the fundamental mode in a multimode fiber," Opt. Lett. **34**(15), 2369–2371 (2009).
14. J. Kerttula, V. Filippov, V. Ustimchik, Y. Chamorovskiy, and O. G. Okhotnikov, "Mode evolution in long tapered fibers with high tapering ratio," Opt. Express **20**(23), 25461–25470 (2012).
15. M. Yu. Koptev, E. A. Anashkina, K. K. Bobkov, M. E. Likhachev, A. E. Levchenko, S. S. Aleshkina, S. L. Semjonov, A. N. Denisov, M. M. Bubnov, D. S. Lipatov, A. Yu. Laptev, A. N. Gur'yanov, A. V. Andrianov, S. V. Muravyev, and A. V. Kim, "Fibre amplifier based on an ytterbium-doped active tapered fibre for the generation of megawatt peak power ultrashort optical pulses," Quantum Electron. **45**(5), 443 (2015).
16. V. Filippov, A. Vorotynskii, T. Noronen, R. Gumenyuk, Y. Chamorovskii, and K. Golantc, "Picosecond MOPA with ytterbium doped tapered double clad fiber," Proc. SPIE **10083**, 100831H (2017).
17. L. Kotov, M. Likhachev, M. Bubnov, O. Medvedkov, D. Lipatov, A. Guryanov, K. Zaytsev, M. Jossent, and S. Février, "Millijoule pulse energy 100-nanosecond Er-doped fiber laser," Opt. Lett. **40**(7), 1189–1192 (2015).
18. I. Pavlov, E. Dülgergil, E. Ilbey, and F. Ö. Ilday, "Diffraction-limited, 10-W, 5-ns, 100-kHz, all-fiber laser at 1.55 μm," Opt. Lett. **39**(9), 2695–2698 (2014).
19. M. Likhachev, S. Aleshkina, A. Shubin, M. Bubnov, E. Dianov, D. Lipatov, and A. Guryanov, "Large-Mode-Area Highly Yb-doped Photodarkening-Free Al_2O_3-P_2O_5-SiO_2-Based Fiber," in *CLEO/Europe-EQEC 2011*, paper CJ.P.24.
20. L. V. Kotov, M. E. Likhachev, M. M. Bubnov, O. I. Medvedkov, M. V. Yashkov, A. N. Guryanov, J. Lhermite, S. Février, and E. Cormier, "75 W 40% efficiency single-mode all-fiber erbium-doped laser cladding pumped at 976 nm," Opt. Lett. **38**(13), 2230–2232 (2013).
21. V. A. Bogatyrev, M. M. Bubnov, E. M. Dianov, A. S. Kurkov, P. V. Mamyshev, A. M. Prokhorov, S. D. Rumyantsev, V. A. Semenov, S. L. Semenov, A. A. Sysoliatin, S. V. Chernikov, A. N. Gur'yanov, G. G. Devyatykh, and S. I. Miroshnichenko, "A single-mode fiber with chromatic dispersion varying along the length," J. Lightwave Technol. **9**(5), 561–566 (1991).
22. V. A. Bogatyrjov and A. A. Sysoliatin, "Efficient method to produce fibers with outer diameter varying along the length," Proc. SPIE **4204**, 274 (2001).
23. Y. Zhu, T. Eschrich, M. Leich, S. Grimm, J. Kobelke, M. Lorenz, H. Bartelt, and M. Jäger, "Yb^{3+}-doped rod-type amplifiers with local adiabatic tapers for peak power scaling and beam quality improvement," Laser Phys. **27**(10), 105103 (2017).
24. R. Paschotta, J. Nilsson, A. C. Tropper, and D. C. Hanna, "Ytterbium-Doped Fiber Amplifiers," IEEE J. Quantum Electron. **33**(7), 1049–1056 (1997).
25. V. A. Bagan, S. A. Nikitov, Yu. K. Chamorovskii, and A. D. Shatrov, "Studying the properties of double-clad active cone optic fiber," J. Commun. Technol. Electron. **55**, 1154 (2010).
26. G. P. Agraval, *Nonlinear Fiber Optics*, P. F. Liao, P.L. Kelley, eds. (Academic Press, 1989).
27. C. Jauregui, J. Limpert, and A. Tünnermann, "Derivation of Raman treshold formulas for CW double-clad fiber amplifiers," Opt. Express **17**(10), 8476–8490 (2009).
28. M. A. Mel'kumov, I. A. Bufetov, K. S. Kravtsov, A. V. Shubin, and E. M. Dianov, "Lasing parameters of ytterbium-doped fibres doped with P_2O_5 and Al_2O_3," Quantum Electron. **34**(9), 843–848 (2004).
29. A. Andrianov, E. Anashkina, S. Muravyev, and A. Kim, "All-fiber design of hybrid Er-doped laser/Yb-doped amplifier system for high-power ultrashort pulse generation," Opt. Lett. **35**(22), 3805–3807 (2010).
30. R. Adair, L. Chase, and S. Payne, "Nonlinear refractive-index measurements of glasses using three-wave frequency mixing," J. Opt. Soc. Am. B **4**(6), 875–881 (1987).
31. C. Pierre, G. Guiraud, C. Vinçont1, N. Traynor, G. Santarelli, and J. Boullet, "120W single frequency laser based on short active double clad tapered fiber," CLEO/Europe - EQEC 2017: Conference Digest, paper CJ-9.3 (25–29 June 2017, Munich, Germany).

1. Introduction

The chirped-pulse amplification technique is now a routine approach to generate high-peak-power femtosecond pulses in Yb-doped fiber lasers. Since very high stretching/compression ratios of about 6000 with a help of diffraction gratings [1] and of about 1000 with a help of monolithic stretcher and a compact compressor [2] were demonstrated, the further peak power scaling is limited mainly by the characteristics of the Yb-doped fiber used in the final amplifier stage. The best results so far were achieved with the help of photonic crystal fibers (PCF), a peak power in the MW range directly from amplifier and more than a few GW of peak power after compression of the chirped pulses [1]. However, large mode area (LMA) Yb-doped PCFs are notorious for their extremely high bend sensitivity and their impossible integration into conventional fiber systems by fusion splicing, resulting in huge dimensions

and non-monolithic designs. Moreover, the complicated technology behind the production of LMA Yb-doped PCFs results in its high cost. To overcome these drawbacks, much effort has been directed towards developing and testing novel LMA fiber designs. To date, many structures have been proposed: leakage channel fibers [3], fibers operating at high-order modes [4], step-index fibers with a microstructured cladding for suppressing high-order modes [5], helical-core fibers [6], chirally coupled core fibers [7], photonic bandgap fibers [8, 9] and other promising designs. However, no results comparable to those obtained with LMA Yb-doped PCFs have been reported. For example, in the case of monolithic chirped pulse amplifiers, the highest peak power does not exceed a few tens kW directly after the amplifier and 10MW after compression [2, 10, 11].

Recently, a novel promising design of LMA Yb-doped tapered fiber has been developed that allows the creation of compact and robust all-fiber systems with low bend sensitivity and simple power scaling [12–16]. This approach is quite simple: the core and cladding diameters monotonically increase along the fiber length to several times their original size. The fundamental mode LP_{01}, excited at the single-mode (thin) end, propagates towards the thick end of the tapered fiber adiabatically without exciting high-order modes (HOMs) [13]. In [14], the passive tapered fiber with an output D_{core}, of 110 μm was produced and adiabatic propagation of the LP_{01} mode along the tapered fiber was demonstrated.

Recently, we demonstrated an active tapered fiber-based chirped pulse amplification (CPA) system that generated 100 kW of peak power in 7-ps pulses centered at 1040 nm, with possibility of compression down to 130 fs [15]. It is also worth to mentioning Ref [16], where amplification of non-chirped 25-ps pulses in a 4-m long tapered fiber with the output core diameter as large as 100 μm was studied. At a high repetition rate (4 MHz) the peak power up to 50-100 kW was demonstrated with a small power level in the 1st Raman Stokes (less than a few percents). A further increase of the peak power up to ~400 kW was accompanied by the appearance of a strong parasitic signal in the Raman Stokes (>60% relative to the net power). In the same paper achieving of 5-MW peak power was reported at 20-kHz repetition rate, but it was accompanied by a very high level (> 80%) of amplified spontaneous emission (ASE), which is inadmissible for most applications. In reality the reported peak power of 5 MW might be significantly overestimated as authors calculate the peak power based on direct detection of the pulse energy by means of an energy meter. This measuring technique can be misleading since the ASE signal is not a strictly continuous wave due to its time-dependent buildup [17, 18]. Special techniques like integrating photodetector [17] or time-domain characterization [18] must be used to evaluate the ASE content.

The present report is devoted to an optimized design of the tapered fiber and the study of a novel operation regime that achieves a high peak power. The chirped pulse amplification achieved power levels up to the sub-MW range directly from the tapered fiber amplifier (comparable to that of PCF-based systems) and further pulse compressions down to sub-ps durations were demonstrated. Special attention was paid to the characterization of the amplified and compressed pulses using various techniques (autocorrelation, FROG, integrating photodetector and independent estimation of the peak power by the self-focusing experiments), which confirmed a low ASE level and a high peak power.

2. Tapered fiber design and fabrication

Similar to [15], the fiber core was made of a photodarkening-free $P_2O_5/Al_2O_3/SiO_2$ (PAS) glass matrix with excess phosphorous, which allowed us to achieve a relatively low core numerical aperture (NA) of ~0.095 and a high Yb_2O_3 content of 2 wt% [19]. To achieve an extremely flat refractive index profile (RIP) the Modified Chemical Vapor Deposition (MCVD) technique was used to deposit all the dopants from the gas phase. $SiCl_4$, $POCl_3$, $AlCl_3$ and $Yb(thd)_3$ (thd = 2,2,6,6-tetramethyl-3,5-heptanedionate) were used as precursors. The $AlCl_3$ and $Yb(thd)_3$ precursors were solid at room temperature, were heated in excess of 100°C to obtain a sufficiently high vapor pressure, and were delivered into the reaction zone through separate heated lines. Such modification resulted in perfect control over the composition and refractive index of each deposited layer (up to ten layers were deposited to

form the core). The flatness of the resultant active core was enough to achieve a perfect Gaussian beam shape of the fundamental mode, up to core diameter of 60-80 μm. The high purity of the PAS glass produced with this technique had essential features compared with those made by solution-doping or powder techniques — gray losses below 30 dB/km were achieved in the fabricated fibers.

An important modification to the design of the fiber was the utilization of the so-called W-shaped RIP. Similar to [20], a depressed layer was deposited just outside the core (see RIP in Fig. 1(a)), which reduced the cut-off wavelength for the core with a fixed diameter and NA. It allowed us to achieve a single-mode propagation regime (the cutoff wavelength was ~980 nm) at the thin end of the tapered fiber, where the core diameter was approximately 10 μm.

The fiber had an outer cladding of fluorine-doped silica with a NA of 0.28. The diameters of the first (pure silica) and the secondary (F-doped) claddings were 71 μm and 85 μm, respectively, at the thin end. To ensure a perfect pump mixture the non-circular first cladding was fabricated prior to the F-doped overcoat. A cross section of the fiber is shown in Fig. 1(b). These factors enabled it to achieve a record high small-signal cladding absorption of 24 dB/m at 976 nm and 6.5 dB/m at 915 nm (see Fig. 1(c)). Another important advantage of the F-doped silica cladding was the simplicity of preparing the thick end, which could be glued into an adapter and angle-polished using standard equipment. Thus, a perfect angle-cleaved thick fiber end compatible with a high power end-pumping technique could be routinely obtained.

Boron-doped stress rods were introduced into the first cladding to create birefringence. The diameter of the rods were higher than those in [15], which allowed us to achieve a polarization extinction ratio of more than 20 dB (measured in the unpumped tapered fiber with a wideband source near 1080-1090 nm).

To produce the tapered fiber, we utilized a non-stationary fiber drawing process. This method was proposed and realized for the first time at FORC RAS in 1991 [21]. It was used to draw relatively long (10-1000 m) tapered fibers. Later, this method was modified to draw short (~1 m in length) tapered fibers [22]. After additional modifications, the non-stationary fiber drawing process allowed us to obtain a highly reproducible set of few tens tapered fibers with a variation in the parameters of less than 10%, with a tapered region length of less than 1 meter and a tapered ratio of more than 7. The diameter distributions of the core, first cladding and second cladding over the fiber length for a tapered fiber cut from such a drawing are presented in Fig. 1(d). The maximum core diameter was 62 μm, the fundamental mode field diameter (MFD) was estimated to be 36.3 μm at 1064 nm.

A smooth enough transition between the thin and the thick ends of the tapered fiber is required for the adiabatic transformation of the fundamental mode during its propagation to the thick end while avoiding the excitation of HOMs. For example, a local taper fabricated with the help of a Vytran splicing system does not allow obtaining M^2 better than 3.5 [23]. The situation is completely different in our case, when the tapered section was produced during drawing and was long enough. The latter was confirmed by measuring the beam quality factor M^2 at the output of the fabricated 2-meter-long tapered fiber. In the experiment, a continuous wave signal at 1064 nm was coupled into the thin end and amplified to 10 W in the tapered fiber, which was pumped through the thick end by a 976 nm multi-mode diode (in all the experiments, the fiber was counter-pumped through the thick end). The M^2 was measured with a Thorlabs M2MS-BC106VIS measurement system and found to be 1.08/1.05 (see Fig. 2).

Optics EXPRESS

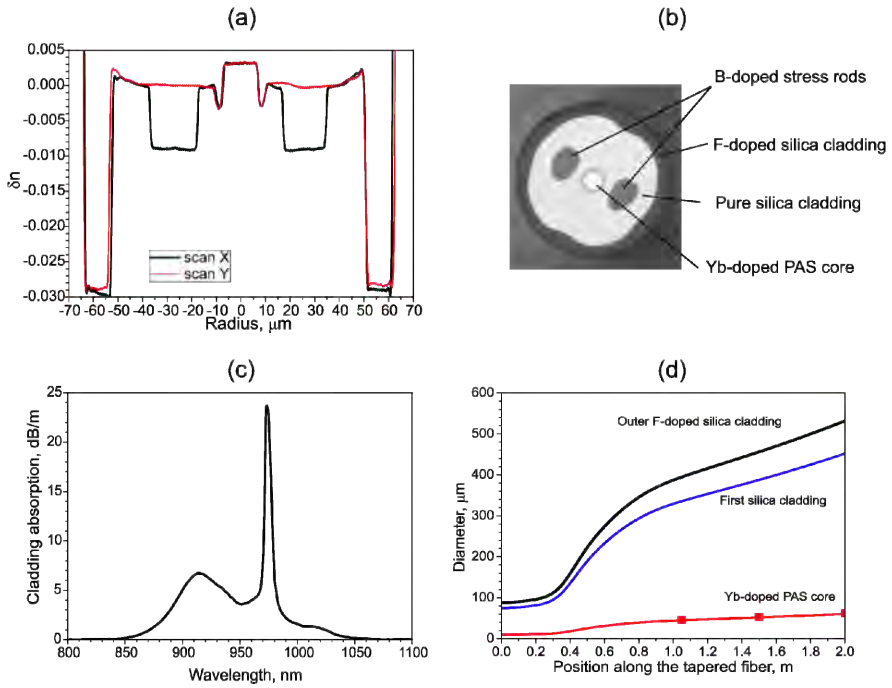

Fig. 1. (a) Measured refractive index profile of a fiber with an outer diameter of 125 μm. (b) Image of the fabricated fiber's cross section. (c) Small-signal absorption from the cladding, measured in the fabricated tapered fiber. (d) Typical dependence of the outer diameter (black curve), first cladding diameter (blue curve) and core diameter (red curve) on the length in the fabricated tapered fiber. Red closed squares depict the value of output core diameter for 1.05-, 1.5- and 2-meter-long tapered fibers.

3. Theoretical analysis

First, a theoretical analysis of the performance of the counter-pumped tapered fiber amplifier was conducted (where the pump power was coupled into the thick end and the signal power was coupled into the thin end). The aim of the analysis was to determine an optimal configuration in terms of a high threshold of nonlinear effects. The modeling was performed by solving the standard rate equations for a quasi two-level system, including forward and backward amplified spontaneous emission (ASE) and the first Raman component [24]. The change in the pump radiation NA during propagation along the tapered fiber and the corresponding pump power leakage was considered according to [25]. The feature of filtering of backward ASE (i.e. propagating from thick to thin end of the tapered fiber) [12] was also considered. Additionally, we accounted for the changes in the mode field diameter of the radiation propagating in the core along the fiber. The absorption cross-sections for the PAS fiber were estimated based on the measured absorption spectra and the ytterbium oxide concentration, as determined by X-ray microanalysis performed using a JEOL 5910LV electron microscope at the Analytical Center of FORC RAS. The emission cross-sections were estimated based on the measured luminescence spectrum and the lifetime of Yb^{3+} ions in the samples of the investigated tapered fibers using the Füchtbauer-Ladenburg equation.

The tapered fiber was considered as a set of short, uniform parts (~1000 pieces), with core and cladding diameters that changed according to the distribution shown in Fig. 1(d). For calculations, the length of tapered fiber was varied by "cutting" some length from the thick end, i.e., a tapered fiber with a length of L was identical to those in Fig. 1(d) that spanned from 0 cm to L. In the experiments, three tapered fibers with lengths of 1.05 meters, 1.5 meters and 2 meters were cut from different periods of the drawn fiber. The results of the calculations were verified experimentally using these three tapered fibers.

Optics EXPRESS

3.1 Saturation signal power in active tapered fibers

It is well known from conventional fibers that decreased input signal can noticeably increase the threshold of nonlinear effects. However, the input signal should be high enough to saturate the amplifier and obtain a high pump conversion efficiency. Most designs for LMA fibers with constant core and cladding diameters over the fiber length give significantly reduced intensities for the signal (due to increases in the mode field area) and the pump (as a typical first cladding diameter in most LMA fibers is increased to 200–400 μm) compared to conventional double clad single-mode Yb-doped fibers. Further shortening of the amplifier length to increase the threshold of non-linear effects results in a small net fiber gain and therefore a high input signal power is required to saturate the amplifier. Typically, saturating such an amplifier requires input signals in excess of hundreds of mW [1].

This behavior was completely different in the tapered fiber amplifiers. Our modeling showed a decrease in the seed signal power required to saturate the amplifier by orders of magnitude compared to conventional LMA fibers (see Figs. 3(a) and 3(b), top pictures). We modeled the operation of different fibers counter-pumped with 25 W at 976 nm. The tapered fibers had lengths of 1.05 meters for 1030 nm signal and 2 meters for 1064 nm signal. For comparison, we calculated the performance of regular fibers, fibers with the same length but constant core and cladding diameters equal to those at the thick end of the tapered fiber. The power required to saturate the amplifier (i.e., to obtain ~70-80% of the maximum output power) is two orders of magnitude higher in the regular fibers than in the tapered fibers.

Our experiments on continuous-wave signal amplification supported the results of our calculations (see Figs. 3(a) and 3(b), bottom pictures). We compared a 1.05-meter-long tapered fiber with core/first-cladding diameters of 10/73 μm at the thin end and 46/338 μm at the thick end with a regular fiber of the same length and with core/first-cladding diameters of 46/338 μm. Additionally, we compared a 2-meter-long tapered fiber (10/73 μm to 62/450 μm) with a 2-meter-long regular fiber with core/first-cladding diameters of 62/450 μm. The regular fibers have the same core/cladding diameters ratio as the tapered fibers (note that the fact that the regular fibers tested were operating in a few mode regime did not influence the amplifier saturation signal power). The tapered fibers had very low saturation signals (below a few mW) without any sign of ASE or self-lasing, while the regular fibers of the same length required saturation signals of two orders of magnitude higher.

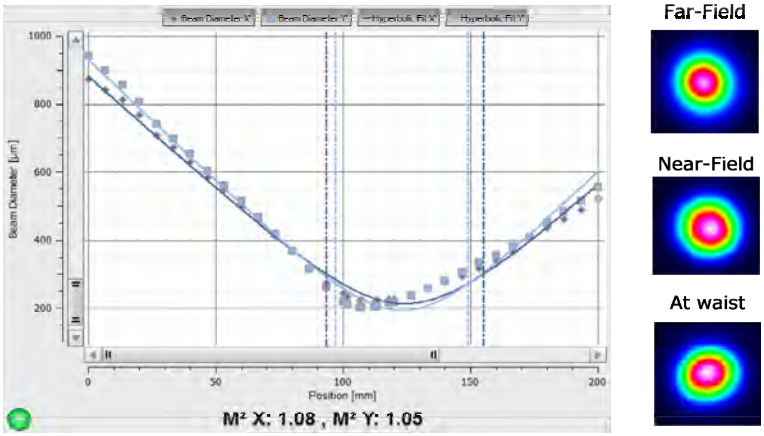

Fig. 2. (c) Caustic measurement for a 2-meter tapered fiber operating at 1064 nm with an average power of 10 W at the far-field (taken way above Rayleigh length), at the near-field (taken between the beam waist and the Rayleigh length) and at the waist beam intensity distributions. Insets were cropped from original images.

Optics EXPRESS

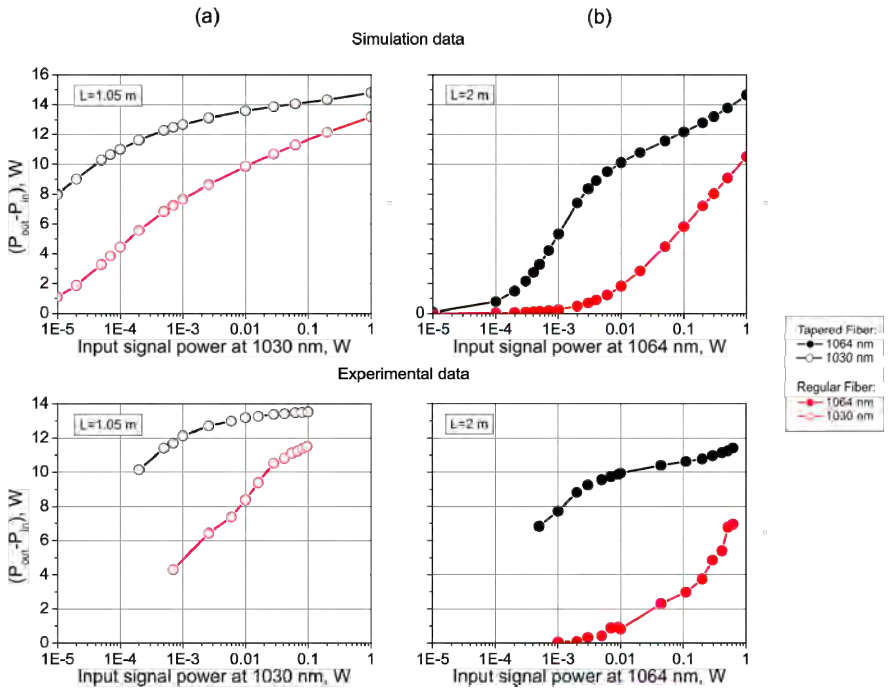

Fig. 3. The calculated and experimentally obtained saturation curves for (a) the 1.05-meter-long tapered fiber and a comparable regular fiber and (b) the 2-meter-long tapered fiber and a comparable regular fiber. The pump wavelength was 976 nm and the power was 25 W. The tapered fiber had core/first-cladding diameters of 10/73 μm at the thin end and 46/338 μm at thick end for the 1.05-meter fiber and 62/450 μm for 2-meter fiber. The regular fibers in the simulations had core/first-cladding diameters of 46/338 μm for the 1.05-meter fiber and 62/450 μm for 2-meter fiber. Regular fibers in the experiments had core/first-cladding diameters of 30/220 μm for the 1.05-meter case and 56/410 for the 2-meter case.

This behavior can be explained by the fact that the pump radiation intensity was greatly increased near the thin end of the tapered fiber compared to the regular fiber. The pump NA used in the experiment was specified to be within 0.22, but direct measurements of the power distribution over the NA shows that more than 90% of the pump power was contained within NA = 0.13 (which we used in our calculations). The first cladding NA was approximately 0.28 and our estimations showed that the leakage loss did not exceed 4 dB up to the thin end of the 1.05-meter tapered fiber or 6 dB for the 2-meter-long tapered fiber. At the same time, the first cladding area decreased by 20-40 times (13-16 dB) near the thin end and the unabsorbed pump intensity increased proportionally. Due to the filtering effect of backward ASE, it sufficiently leaks from the active core at the transition region, preserving inversion level in thin part to depleting by signal. Moreover, the signal intensity was higher by an order of magnitude at the thin (signal input) end of the tapered fiber as compared to that of a regular fiber, as it propagated in a 10 μm core compared to the 40..60 μm core of the regular fiber. As a result, the unabsorbed pump was efficiently converted into signal without the generation of ASE, and the minimum signal required to saturate the amplifier was orders of magnitude less than that of the regular fiber.

3.2 Threshold of stimulated Raman scattering (SRS) in a tapered fiber amplifier

In fiber-based chirped pulse amplification systems, there are two main factors that limit the maximum peak power at the output. The smallest threshold has a self-phase modulation (SPM) effect; however, this restricts the quality of further pulse compression, and not the maximum achievable peak power level at the amplifier output. The second nonlinear effect is stimulated Raman scattering (SRS), which leads to a power transfer from the amplified pulse

to the first Stokes component shifted by approximately 440 cm^{-1} [26]. For an amplifier operating at 1030 nm, the first Stokes component is centered at approximately 1080 nm, and in the case of a 1064 nm operating signal, the first Stokes component is centered at 1125 nm.

In this study, we calculated the SRS threshold by directly solving the rate equation, which included a seed due to thermal-induced photons [27] at the first Stokes wavelength and ASE generated in the amplifier at this wavelength. The SRS threshold was set at the amplification of the SRS signal at the first Stokes wavelength to more than 1% of the main signal.

We estimated the SRS thresholds for the tapered fiber amplifier operating at either 1030 or 1064 nm with 10 mW of input power and pumped with either a 915 or 976 nm multimode diode. The tapered fiber length was varied from 0.6 to 2 meters. In addition to the tapered fiber, we modeled a PCF fiber with core/cladding diameters of 40/200 μm (DC-200/40-PZ-Yb from NKT Photonics), which the absorption and emission cross-sections and the lifetime of ytterbium ions were taken from [28].

The results of the calculations, shown in Fig. 4(a), were very unusual. The SRS threshold for the PCF was inversely proportional to the fiber length, as expected. In contrast, the SRS threshold for the tapered fiber increased with the fiber length. The tendency was the most apparent in the case of a 1064 nm signal with a 976 nm pump, where the SRS threshold increased from 148 kW to 301 kW as the tapered fiber length is increased from 1.05 to 2 meters.

This effect cannot be explained solely by the considerable increase in the MFD at the output of the tapered fiber as its length was increased. The cause for this phenomenon is apparent in Fig. 4(b), which shows that in the case of 976 nm pumping, the 1064 nm signal propagated along the first meter of the fiber without any gain or loss, whereas the 1030 nm signal showed some absorption, and in the last 0.8-1 meters of the fiber, where the MFD is high, the signal experienced a very high gain. As a result, the accumulated nonlinearity was very small. This behavior was caused by the fact that for the 2-meter fiber, the small-signal absorption at 976 nm exceeded 50 dB; thus, only a small part of the pump power reached the thin end of the fiber. Near the thick end of the tapered fiber, the growth of the signal was defined mainly by the pump absorption rate, which was very high because of the high Yb^{3+} content. The low signal saturation power in the tapered fiber amplifier (see previous paragraph) resulted in a low level of forward ASE in this regime. It is interesting to note that this propagation regime is a specific feature of the tapered fiber caused by the small MFD at the thin tapered fiber section. Our calculations show that in the case of a regular fiber with a similar clad absorption, the SRS threshold slowly decreases with fiber length.

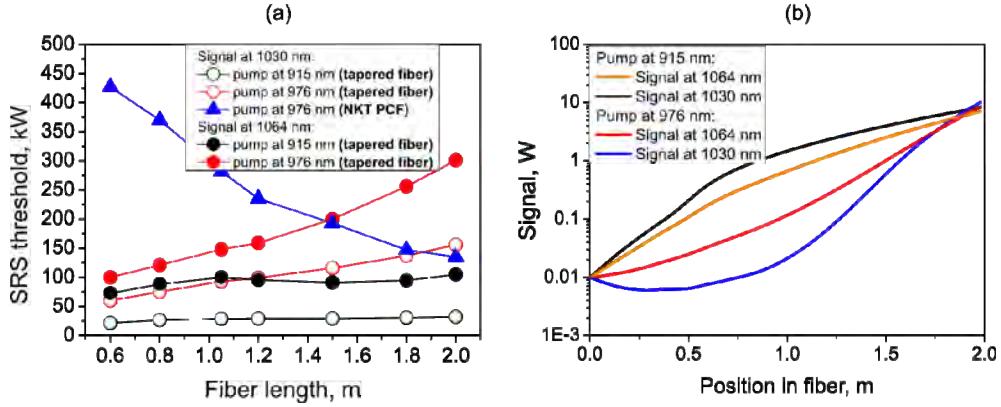

Fig. 4. (a) Calculated SRS threshold dependence on the length of the tapered fiber or the PCF (signal power = 10 mW, pump NA = 0.13). (b) Calculated signal distribution over the length of a 2-meter tapered fiber.

It should be noted that the SRS threshold was calculated to be much smaller at 1030 nm than that of the 1064 nm signal. This feature was caused by ASE in the 1080 nm region that

was generated by the tapered fiber amplifier, which acted as a seed for SRS. Moreover, there was additional gain in the first Stokes signal near 1080 nm due to the Yb^{3+} ions. The situation was completely different in the case of the 1064 nm signal, where both the ASE generated at the first Stokes wavelength (1125 nm) and the gain due to the Yb^{3+} ions were orders of magnitudes smaller.

Thus, our calculations predicted a new amplification regime, which allowed us to realize a very high threshold for nonlinear effects, particularly SRS. The use of a signal near 1064 nm (or any other wavelength whose 1st Stokes wavelength lies outside the amplification band of Y^{3+} ions) and a 976 nm pump were required to realize this regime. A relatively long Yb-doped tapered fiber length with a net small-signal clad absorption of approximately 50 dB at the pump wavelength were also necessary. For these conditions, a sub-MW SRS threshold was predicted in the fabricated Yb-doped tapered fiber.

4. Experiments

4.1 Experimental set-up

To verify the calculations, we realized the laser scheme depicted at Fig. 5. In the first set of experiments, our aim was to estimate the SRS threshold in the different amplifier configurations (tapered fiber length, signal wavelength). Picosecond narrow-bandwidth seed sources from Fianium were used (13 ps at 1030 nm and 5 ps at 1064 nm). Generated pulses were amplified in a low-power "Yb:1" amplifier, reduced in repetition rate by an acousto-optical modulator (AOM) down to 1 MHz, and amplified again in a low-power "Yb:2" amplifier up to an average power of 10 mW. The pulses duration at the tapered fiber input were 18 ps in the case of 1030 nm seed and 8 ps in the case of 1064 nm seed. These pulses were further amplified in the active tapered fiber, whose input end was spliced to the output of "Yb:2". The output end of the tapered fiber was angle-polished to 8 degrees to avoid self-lasing. To properly align this end, we used a translation stage that provided five axes of adjustment (x, y, z, yaw and pitch). As light came out of the angle-polished end of the tapered fiber at an angle of approximately 12° relative to the fiber axis, the fiber was rotated to align incident light direction and the axis of the optical scheme. The tapered fiber was counter-pumped by a wavelength-stabilized (976 ± 0.5 nm) fiber-coupled diode laser that provided up to 50 W of output power within a NA of 0.13. The ASE at the output of the tapered fiber was measured using the so-called "integrating photodetector" [17] (see details in the Appendix).

4.2 Pump-to-signal conversion efficiency in the tapered fiber amplifier

First, we measured the pump-to-signal conversion efficiency in three different lengths of tapered fibers (1.05, 1.5 and 2 meters) and different signal wavelengths (1030 and 1064 nm). The signal power was set to 10 mW, and the repetition rate was 1 MHz. The results are shown in Table 1.

Table 1. The tapered fiber-based amplifier pump-to-signal conversion efficiency

Taper length, m	Efficiency for the signal at 1030 nm@10 mW, %	Efficiency for the signal at 1064 nm@10 mW, %
1.05	61	53
1.5	53	54
2	-	51

Optics EXPRESS

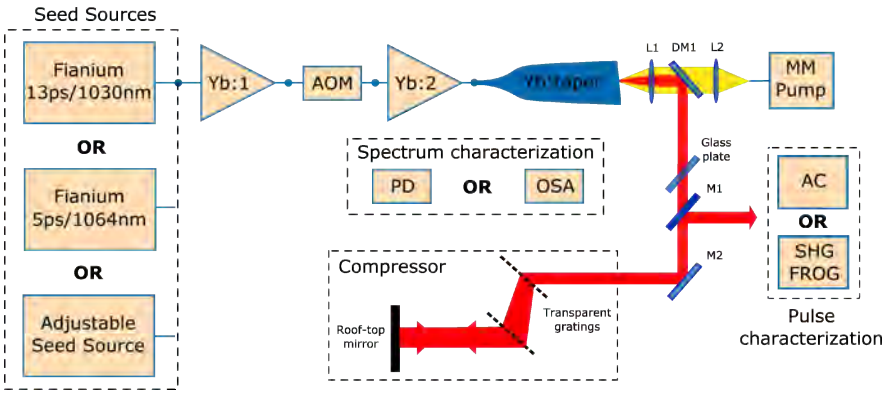

Fig. 5. The experimental setup for the chirped pulse amplification. Yb:1 and Yb:2 are low power single-mode core-pumped amplifiers; AOM: acousto-optic modulator; L1, L2: aspheric lenses, f = 11 mm; DM1: dichroic mirror, HR@1064 nm, HT@976 nm; M1, M2: mirrors; Pump: multi-mode wavelength-stabilized pump diode 976@50 W; PD: integrating photodetector; OSA: optical spectrum analyzer; AC: optical autocorrelator; SHG FROG: second harmonic generation frequency-resolved optical gating set-up.

As can be seen in Table 1, the differential efficiency remained almost the same across the different fiber lengths. However, in the case of the 2-meter-long tapered fiber operating at 1030 nm, the ASE level near 1064 nm was so high that this fiber could not be used for amplification of a 1030 nm signal. In the case of the 1.05-meter-long fiber operating at 1064 nm, we also obtained a high ASE near 1030 nm, but its level was at acceptable level of a few percent. Note, that the pump-to-signal conversion efficiency shown in the Table 1 can be somewhat increased if a higher input signal power is coupled into the amplifier.

4.3 SRS threshold in the tapered fiber amplifier

As mentioned above, the tapered fibers require very low signal powers to reach the saturation regime. Thus, to determine the minimal acceptable level of the input signal power, we measured the SRS threshold dependence on the input signal power. Additionally, we measured the amount of ASE in the output beam of the system. Measurements were performed with a 1.05-meter-long tapered fiber operating at 1030 nm (Fig. 6(a)) and for a 2-meter-long tapered fiber operating at 1064 nm (Fig. 6(b)). The SRS threshold was estimated by measuring the output spectrum of the amplified signal from the tapered fiber and evaluating the ratio of the power of the first Stokes component to the power of the whole spectrum. For the 1064 nm signal, this method is easy to use because the first Stokes component was far away from the ASE of the Yb^{3+} ions. However, for the 1030 nm signal, the first Stokes component was centered at 1080 nm, which overlaps with the ASE spectrum, making it difficult to obtain accurate measurements of the SRS component. The measured SRS threshold was varied within 30% from experiment to experiment due to variations in the coupled pump NA (due to inaccuracy in the rotational adjustments of the fiber). The pump NA defines the pump loss distribution and in this way affects the signal distribution along the tapered fiber length as well as SRS threshold.

As shown in Fig. 6, the SRS threshold grew quickly as the input signal power decreased. The amount of ASE exhibited the same behavior. Thus, with an input signal power of a few mW, it was possible to achieve a high peak power with an acceptably low amount of ASE at the output of the system.

The SRS threshold was measured for all the available tapered fibers with a 10 mW input signal, and the results are shown in Table 2. The results agreed in general with our theoretical calculations. In the case of using a 1030 nm signal, a high level of ASE lead to decrease of the SRS threshold with increase of the tapered fiber length, and for the 2-meter tapered fiber it was even impossible to estimate the threshold because of an extremely high amount of ASE. In contrast, for the 1064 nm signal, the highest SRS threshold was observed with the 2-